Virtual Resource Allocation in Virtualized Small Cell Networks with Physical-Layer Network Coding Aided Self-Backhauls

Yulun Cheng*, Longxiang Yang and Hongbo Zhu
Jiangsu Key Lab of Wireless Communications
Nanjing University of Posts and Telecommunications
Nanjing, P. R. China. 210003
[e-mail: chengyuluen@163.com]
*Corresponding author: Yulun Cheng

Received June 19, 2016; revised September 27, 2016; revised December 23, 2016; accepted April 25, 2017; published July 31, 2017

Abstract

Virtualized small cell network is a promising architecture which can realize efficient utilization of the network resource. However, conventional full duplex self-backhauls lead to residual self-interference, which limits the network performance. To handle this issue, this paper proposes a virtual resource allocation, in which the residual self-interference is fully exploited by employing a physical-layer network coding (PNC) aided self-backhaul scheme. We formulate the features of PNC as time slot and information rate constraints, and based on that, the virtual resource allocation is formulated as a mixed combinatorial optimization problem. To solve the problem efficiently, it is decomposed into two sub problems, and a two-phase iteration algorithm is developed accordingly. In the algorithm, the first sub problem is approximated and transferred into a convex problem by utilizing the upper bound of the PNC rate constraint. On the basis of that, the convexity of the second sub problem is also proved. Simulation results show the advantages of the proposed scheme over conventional solution in both the profits of self-backhauls and utility of the network resource.

Keywords: Virtual resource allocation, wireless virtualization, small cell, wireless self-backhauls, physical-layer network coding

This work was supported by the National Basic Research Program of China (973 Program) under Grant No. 2013CB329104, and the National Natural Science Foundations of China under Grants No. 61601238, No. 61372124 and No. 61427801.

https://doi.org/10.3837/tiis.2017.08.005 **ISSN : 1976-7277**

1. Introduction

Following its success in reducing the capital and operation expenses, wireless virtualization [1-2] has been regarded as one of the distinct features of future wireless networks. By abstracting and slicing physical wireless network infrastructure and spectrum resources, wireless virtualization decouples the network resources from the infrastructure providers (InP). These virtualized network resources can be shared by multiple mobile virtual network operators (MVNOs), which provide diverse services to the users. Thus, it enables multiple MVNOs to coexist on the same physical network and share the network resources, which is significant to reduce their capital and operation expenses [3]. Due to the potential benefits, many works have focused on the virtualization of wireless networks. For example, in [4], a virtualization scheme for long-term evolution (LTE) was proposed, in which the eNB and physical resource block were virtualized and shared. In [5], the virtualization with device-to-device communication underlying LTE networks was investigated. Moreover, virtualization for WiMAX [6], wireless optical networks [7], and wireless local area networks [8] were also studied. However, these works only involved virtualization without further extension.

Besides virtualization, another emerging solution for next generation wireless network is small cell [9-10]. Small cell is an economical solution to providing high-quality coverage to data-enabled smartphone users that are not close to a cell site, and more and more wireless operators now depend on this emerging technology to provide service for high-speed data and voice applications. In small cell, although some wired [11] and wireless [12] schemes have been proposed, backhauls are still the bottleneck because of the high deployment expense.

Recently, wireless self-backhauls [13-14] have been considered as an efficient solution to the backhauls issue of small cell. By easing connectivity of the nodes, wireless self-backhauls enable better coverage and reachability of the networks. Therefore, small cells with wireless self-backhauls have drawn huge attentions from both academic and industry.

Since wireless virtualization and self-backhauled small cell are both promising for the next generation wireless networks, the combination of them may bring considerable promotion to the network performance. From this perspective, the authors in [15] have made commendable attempt, and proposed a virtual resource allocation for the virtualized small cells with self-backhauls. However, even when the utilization of the network resource was improved, the backhauls issue is still critical. In [15], although full duplex (FD) [16] was employed to reduce the expense of self-backhauls, it demonstrated that the residual self-interference was destructive to the utility of the network resource.

In fact, the residual self-interference is caused by the non-ideal interference cancellation [15], because the overlap of the uplink and downlink signals are traded as harmful. Contrary to this conventional concept, the birth of network coding (NC) [17] shows that it is beneficial to transmit the combinations of signal from different sources. Many research works, such as [18-20] have addressed the application of NC in the one-way scenario, and show that the transmission efficiency can be improved. Besides one-way scenario, NC is also able to be applied in two-way scenario, which is named as physical-layer network coding (PNC) [21]. In PNC, the natural overlap of the wireless electromagnetic waves are considered as an efficient coding method to realize network coding, which is in good agreement with the self-backhaul of small cell. Therefore, in order to mitigate the residual self-interference and improve the profits of self-backhauls, we bring the concept of PNC into virtualized small cells with self-backhauls.

In this paper, a PNC-based scheme is proposed to reduce the residual self-interference and improve the profits of backhauls. On the basis of that, the virtual resource allocation is investigated when the virtualization and PNC aided self-backhauls are jointly considered. The major contributions of this paper are summarized as follows.

- A PNC aided self-backhaul scheme is proposed by utilizing the overlap of the uplink and downlink signals, so that the destructive effects of the residual self-interference are mitigated.
- By abstracting the feathers of PNC as time slot and information rate constraints, the virtual resource allocation is formulated as a mixed combinatorial optimization problem. In addition, the fixed power budget constraint is also taken into account.
- To solve the problem efficiently, we decompose the formulated problem into two sub problems. By utilizing the upper bound of the PNC rate constraint, the first sub problem is approximated and transferred into a convex problem. And then, the convexity of the second sub problem is also proved. Based on the results, a two-phase iteration algorithm is developed for the virtual resource allocation.

The rest of the paper is organized as follows. Section 2 presents the system model of virtualized small cell networks with PNC aided self-backhauls. The virtual resource allocation problem is formulated in Section 3. In Section 4, the formulated problem is divided into two sub problems and the corresponding solutions are presented in details. Simulation results are discussed in Section 5. Finally, Section 6 concludes the paper.

2. System Model

In this section, the architecture of the virtualized small cell network is firstly presented. And then, the proposed PNC aided self-backhaul scheme is described.

2.1 Virtualized Small Cell Network

Fig. 1 depicts the architecture of the virtualized small cell networks. As is shown, M InPs coexist in a certain geographical area. Each InP manages one macro base station (MBS) and several small cell base stations (SBSs). Besides, there are N mobile virtual network operators (MVNOs), and through the same substrate networks, each MVNO is able to provide wireless access service to all the users in area i, $i=1,\cdots,M$. The wireless virtualization part is responsible to virtualize the physical resources from the InPs and allocate them among the MVNOs. That is, each InP provides its spectrum, power and base stations, which are virtualized as virtual network resources. Each MVNO leases the virtual network resource from InPs at the deliberated price, and utilize them to serve their users. We assume that the spectrum bandwidth of InP m is $B_m, m=1,\cdots,M$. To avoid the interlayer interference, the spectrum of InP m is divided into $a_m B_m$ and $(1-a_m)B_m$, which are utilized by the MBS and SBSs of InP m, respectively. So the spectrum indicators of the network can be denoted as $\boldsymbol{a}=(a_1,a_2,\cdots,a_M)$. We denote $\boldsymbol{S}_m$ as the set of SBSs owned by InP m, and denote S_m^j as the j-th SBS in $\boldsymbol{S}_m$. Let $\boldsymbol{U}_i$ be the set of users served by MVNO i. Each user can choose a MBS or SBS to get the access service, so $\boldsymbol{U}_m$ and $\boldsymbol{U}_m^{Sj}$ denote the sets of users associated to the MBS and the j-th SBS of InP m, respectively.

Thus, to maximize the total profits of all MVNOs, the wireless virtualization part has to dynamically allocate the access BS and other virtual resource from multiple InPs to different

MVNO users. This problem is also known as virtual resource allocation [15], which is significant for the network efficiency [22] and will be formulated in the next section. To facilitate the problem formulation, we firstly introduce the PNC aided self-backhaul scheme in the next subsection.

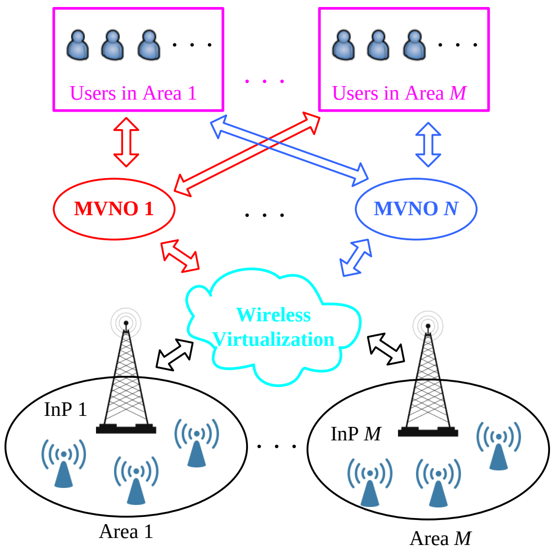

Fig. 1. The architecture of the virtualized small cell network.

2.2 PNC Aided Self-backhaul

In the architecture presented in **Fig. 1**, since many SBSs are deployed, the backhaul expense is heavy for the MVNOs [19]. FD self-backhaul [16] is considered as an economical solution to reduce this expense. As shown in **Fig. 2 (a)**, each SBS is able to receive signal from the MBS while simultaneously transmit to the users on the same frequency band. Thus, the downlink (DL) transmission costs only one time slot (TS), which is equivalent comparing with the direct transmission from MBS to the user. However, due to the less-than-ideal self-interference cancellation in the SBS, the signal-noise ratio of the backhaul DL signal will be degenerated by the access DL signal, which decrease the gain of the solution. The situation is similar for the backhaul uplink (UL) and access UL signals.

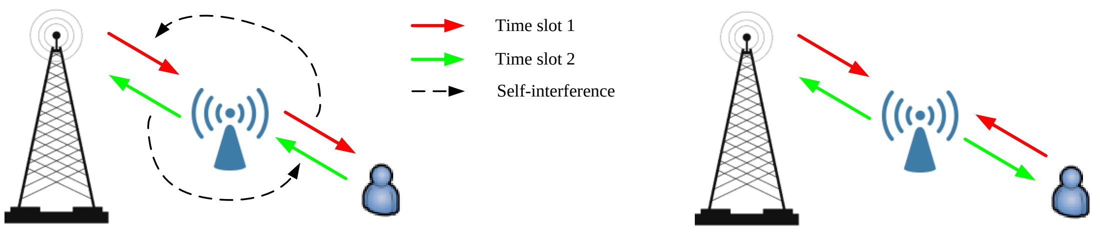

(a) FD-based self-backhaul

(b) The proposed scheme

Fig. 2. PNC aided self-backhaul.

Different from the FD-based self-backhaul, we propose a PNC aided self-backhaul in **Fig. 2(b)**. When user u is associated to S_m^j, the whole transmission consists of 2 TS. In TS 1, for user $u \in \boldsymbol{U}_m^{Sj}$, the MBS m and user u simultaneously transmit signals to SBS S_m^j with the same transmitting power P [21], so the received signal at S_m^j can be written as

$$y_{Sj} = \sqrt{P} h_m^{Sj} x_m + \sqrt{P} h_u^{Sj} x_u + n_{sj}, j \neq 0, \tag{1}$$

where x_m and x_u are the data of MBS m and user u, respectively. n_{sj} denotes the background noise. h_m^{Sj} and h_u^{Sj} denotes the channel gains from MBS m and user u to SBS S_m^j, respectively. Since y_{Sj} is the overlap of the signals from MBS m and user u, it can be naturally regarded as the PNC codeword of SBS S_m^j. In TS 2, SBS S_m^j broadcasts this PNC signal with unit power, so the received signals at MBS m and user u can be expressed as

$$y_m = h_{Sj}^m (\sqrt{P} h_m^{Sj} x_m + \sqrt{P} h_u^{Sj} x_u + n_{sj}) + n_m, \tag{2}$$

$$y_u = h_{Sj}^u (\sqrt{P} h_m^{Sj} x_m + \sqrt{P} h_u^{Sj} x_u + n_{sj}) + n_u, \tag{3}$$

where h_m^{Sj} and h_u^{Sj} denote the channel gains from SBS S_m^j to MBS m and user u, respectively. It is assumed that the channel gain is only known at the receiver. Besides, any channel gain between two nodes is assumed to be constant during a transmission round, since the resource allocation is carried out in the channel coherence time. Also, according to the principle of reciprocity, there are $h_m^{Sj} = h_{Sj}^m$ and $h_u^{Sj} = h_{Sj}^u$ in the transmission round.

Since h_{Sj}^m, P, and x_m are known at MBS m, the received PNC signal is decoded with serial interference cancellation (SIC), so the output of SIC can be written as

$$\begin{aligned} y_m^{\text{SIC}} &= \frac{y_m}{h_{Sj}^m} - \sqrt{P} h_m^{Sj} x_m \\ &= \sqrt{P} h_u^{Sj} x_u + n_{sj} + \frac{n_m}{h_{Sj}^m}. \end{aligned} \tag{4}$$

Similarly, for user u, the output of SIC can be expressed as

$$y_u^{\text{SIC}} = \sqrt{P} h_m^{Sj} x_m + n_{sj} + \frac{n_u}{h_{Sj}^u}. \tag{5}$$

Then MBS m and user u can extract their desired information from y_m^{SIC} and y_u^{SIC}, respectively.

Comparing with the FD-based self-backhaul in **Fig. 2 (a)**, the TS cost is equivalent for PNC aided self-backhaul. However, there are two distinct differences between these two solutions. Firstly, different from the FD-based self-backhaul, there is no interference cancellation operation at SBS for the proposed scheme. In stead, the SBS only forwards the received signals, which brings no residual self-interference. Secondly, PNC decoding are required at

MBS and users in the proposed scheme, and since the signal forwarded by SBS is considered as PNC codeword, it also brings no residual self-interference according to (4) and (5). These two distinct differences enable the superiority of the proposed scheme.

In the presented network, the wireless virtualization part is responsible to allocate the access BS and other virtual resource to each $u \in \boldsymbol{U}_i$. So let $x_u^{m,j}$ denotes the access BS indicator of user u. When user u is accessed through one certain BS, $x_u^{m,j}=1$, otherwise $x_u^{m,j}=0$. Besides, $x_u^{m,j}(j \neq 0)$ means user u is accessed through SBS S_m^j, while $x_u^{m,0}$ means it is accessed through MBS m. We denote $y_u^{m,j}$ as the TS ratio allocated to user u. Similarly, $y_u^{m,0}$ and $y_u^{m,j}$ denote the TS ratio occupied by user u from MBS m and SBS S_m^j, respectively.

We focus on the achievable rate of the DL, since it usually has more traffic than the UL. Let $R_u^{m,j}$ denotes the achievable rate of user u from DL. For the user $u \in \boldsymbol{U}_m$, let P_m denote the transmitting power of MBS m, so $R_u^{m,0}$ can be expressed as

$$R_u^{m,0} = a_m B_m \log(1+\frac{P_m |h_u^m|^2}{\sigma^2}), \tag{6}$$

where h_u^m is the channel gain between user u and MBS m. σ^2 is the variance of the background noise, which follows the standard Gaussian distribution. For the user $u \in \boldsymbol{U}_m^{Sj}$, according to (5), $R_u^{m,j}$ can be expressed as

$$R_u^{m,j} = (1-a_m) B_m \log(1+\frac{P |h_m^{Sj}|^2}{(1+\frac{1}{|h_{Sj}^u|^2})\sigma^2}). \tag{7}$$

Hence, for a given user, we denote C_u^m as its long-term rate, which can be expressed as

$$C_u^m = x_u^{m,0} y_u^{m,0} R_u^{m,0} + \sum_{j \in \boldsymbol{S}_m} x_u^{m,j} y_u^{m,j} R_u^{m,j}. \tag{8}$$

Besides, for a given SBS S_m^j, we denote R_m^{Sj} as its achievable rate from the PNC signal. Since S_m^j does not deocde the signal, R_m^{Sj} can be bounded by the achievable rate of the single signal, that is

$$R_m^{Sj} \leq (1-a_m) B_m \log(1+\frac{P |h_m^{Sj}|^2}{\sigma^2}). \tag{9}$$

Meanwhile, since all the SBSs owned by one InP share the same frequency band, they are separated in the time domain, so let z_m^{Sj} denote the TS allocated to SBS S_m^j, and its long-term rate can be written as

$$C_m^{Sj} = z_m^{Sj} R_m^{Sj}. \tag{10}$$

The variables used in this paper are listed in **Table 1**.

Table 1. Variable definitions

Variable	Definition
$\boldsymbol{a}$	spectrum allocation indicator vector
$\boldsymbol{S}_m$	the set of SBSs managed by InP m
$\boldsymbol{U}_i$	the set of users served by MVNO i
$\boldsymbol{U}_m$	the set of users associated to the MBS of InP m
$\boldsymbol{U}_m^{Sj}$	the set of users associated to the j th SBS of InP m
P	transmitting power of MBS for $u \in \boldsymbol{U}_m^{Sj}$
P_m	transmitting power of MBS for $u \in \boldsymbol{U}_m$
P_m^T	transmitting power budget of InP m
h_m^{Sj}	channel gain from MBS m to SBS S_m^j
h_u^{Sj}	channel gain from user u to SBS S_m^j
x_m	the data of MBS m
x_u	the data of user u
y_{Sj}	the received signal at SBS S_m^j in TS 1
y_m	the received signal at MBS m in TS 2
y_u	the received signal at user u in TS 2
$x_u^{m,j}$	access BS indicator of user u
$y_u^{m,j}$	TS ratio allocated to user u
z_m^{Sj}	TS ratio allocated to SBS S_m^j
$R_u^{m,j}$	achievable rate of user u from all BSs of InP m
R_m^{Sj}	achievable rate of SBS S_m^j from the PNC signal
C_u^m	sum rate of user u from all BSs of InP m
C_m^{Sj}	achievable rate of SBS S_m^j from backhaul link

3. Problem Formulation

In this section, the virtual resource allocation problem in virtualized small cell network with PNC aided self-backhaul is formulated. Firstly, the utility for the users, MVNOs, and InPs are defined according to the system model of section 2. On the basis of that, the virtual resource allocation problem is formulated to maximize the total utility of all MVNOs.

3.1 Utility Function Definition

The utility function is the metric of the profit, which is the gap between the income and the cost. For user $u \in \boldsymbol{U}_i$, its utility function is denoted as F_u, which is defined as

$$F_u = \sum_{m=1}^{M} \varepsilon C_u^m - \delta_u, \tag{11}$$

where ε is the profit per bit rate, and δ_u is the expense paied by user u for the access service. For simplicity, we assume that $\varepsilon = 1$. For any MVNO i, its utility function can be expressed as

$$F_{MVNO}^{i}=\sum_{m=1}^{M}\sum_{u\in \boldsymbol{U}_i}\delta_u C_u^m-\sum_{m=1}^{M}\gamma_m T_i^m-\sum_{m=1}^{M}Q_i^m, \tag{12}$$

where γ_m denotes the depliberated price for leasing wireless resource between MVNO i and InP m. In practice, to ensure the profits of MVNOs, γ_m and δ_u are usually in defferent orders of magnitude, so it is assumed that $\gamma_m \ll \delta_u$. T_i^m is the metric of spetrum and power resource provided by InP m, which can be written as

$$T_i^m=\sum_{u\in \boldsymbol{U}_m \& u\in \boldsymbol{U}_i} x_u^{m,0}y_u^{m,0}a_m B_m P_m+w_m\sum_{j\in \boldsymbol{S}_m \& u\in \boldsymbol{U}_i} x_u^{m,j}y_u^{m,j}(1-a_m)B_m P, \tag{13}$$

where the product of the power and spetrum is utilized to quantify the wireless resource consumption of MVNO i. w_m is the discount price of SBSs, and to encourage the utilization of SBS, there is $w_m<1$. In (12), the last term is the expense of MVNO i for using self-backhaul resource of InP m, which can be expressed as

$$Q_i^m=\sum_{j\in \boldsymbol{S}_m} g_{PNC}\sum_{u\in \boldsymbol{U}_i \& \boldsymbol{U}_m^{Sj}} x_u^{m,j}y_u^{m,j}R_u^{m,j}, \tag{14}$$

where g_{PNC} represents the resource consumption of the PNC aided self-backhaul and can be written as

$$g_{PNC}=(1-a_m)Pz_m^{Sj}. \tag{15}$$

Hence, the total utility of all the MVNOs can be expressed as

$$\begin{aligned}
F_{MVNO}&=\sum_{i=1}^{N}F_{MVNO}^{i}\\
&=\sum_{i=1}^{N}\{\sum_{m=1}^{M}(\sum_{u\in \boldsymbol{U}_i}\delta_u(x_u^{m,0}y_u^{m,0}R_u^{m,0}+\sum_{j\in \boldsymbol{S}_m}x_u^{m,j}y_u^{m,j}R_u^{m,j})\\
&\qquad -\gamma_m(\sum_{u\in \boldsymbol{U}_m \& u\in \boldsymbol{U}_i}x_u^{m,0}y_u^{m,0}a_m B_m P_m+w_m\sum_{j\in \boldsymbol{S}_m \& u\in \boldsymbol{U}_i}x_u^{m,j}y_u^{m,j}(1-a_m)B_m P)\\
&\qquad -\sum_{j\in \boldsymbol{S}_m}(1-a_m)Pz_m^{Sj}\sum_{u\in \boldsymbol{U}_i \& \boldsymbol{U}_m^{Sj}}x_u^{m,j}y_u^{m,j}R_u^{m,j})\}.
\end{aligned} \tag{16}$$

3.2 Virtual Resource Allocation Problem

To maximize the total utility of all MVNOs, we employ (16) as the objective function, and formulate an optimization problem to decide the BS indicator $\boldsymbol{X}$, TS ratio $\boldsymbol{Y}$, SBS TS ratio $\boldsymbol{Z}$, spectrum indicator $\boldsymbol{a}$, and transmission power $\boldsymbol{P}$. The corresponding constraints are formulated as follows.

Firstly, in accordance with the Shannon theory, processing of a signal will not increase its information. So for any $u\in \boldsymbol{U}_m^{Sj}$, its achievable rate will not beyond the one of S_m^j when MBS m transmits. Hence, by employing the upper bound of (9), the information constraint can be expressed as

$$C1: \quad \sum_{u \in \boldsymbol{U}_m^{Sj}} x_u^{m,j} y_u^{m,j} R_u^{m,j} \le z_m^{Sj} (1-a_m) B_m \log(1+\frac{P\,|h_m^{Sj}|^2}{\sigma^2}), \;\; j \ne 0. \tag{17}$$

Besides, for each user u, it is only accessed either to one MBS or to one SBS, so there are

$$C2: \quad x_u^{m,j} \in \{0,1\}. \tag{18}$$

$$C3: \quad \sum_{m=1}^{M} \sum_{j=0 \text{ or } j \in \boldsymbol{S}_m} x_u^{m,j} \le 1. \tag{19}$$

Thirdly, on time dimension, all the users share the same TS resource of their associated BS, so the TS constraints should be satisfied as

$$C4: \quad 0 \le y_u^{m,j} \le 1, \forall m, j. \tag{20}$$

$$C5: \quad \sum_{u \in \boldsymbol{U}_m} x_u^{m,0} y_u^{m,0} \le 1. \tag{21}$$

$$C6: \quad \sum_{u \in \boldsymbol{U}_m^{Sj}} x_u^{m,j} y_u^{m,j} \le 1. \tag{22}$$

Similarly, for each SBS, the TS constraints are given as

$$C7: \quad 0 \le z_u^{Sj} \le 1, \forall m, j. \tag{23}$$

$$C8: \quad \sum_{j \in \boldsymbol{S}_m} z_m^{Sj} \le 1, \forall m. \tag{24}$$

After that, because PNC is utilized for self-backhaul, the TS symmetry condition [21] should be satisfied, which is

$$C9: \quad \sum_{u \in \boldsymbol{U}_m^{Sj}} x_u^{m,j} y_u^{m,j} = z_m^{Sj}, j \ne 0. \tag{25}$$

Furthermore, for each InP m, the spectrum indicator a_m should satisfies

$$C10: \quad 0 \le a_m \le 1, \forall m. \tag{26}$$

Meanwhile, since its users are seperated on the time dimension, there are at most one MBS and one SBS transmitting simultaneously, so the power constraint can be expressed as

$$C11: \quad P_m + P \le P_m^T. \tag{27}$$

where P_m^T is the fixed power budget of InP m.

With the above constraints, the virtual resource allocation problem with PNC aided self-backhaul can be formulated as

$$\begin{aligned} P1: \quad & \max_{\boldsymbol{X},\boldsymbol{Y},\boldsymbol{Z},\boldsymbol{a},\boldsymbol{P},\boldsymbol{P}_m} F_{MVNO} \\ & s.t. \ \ C1 \sim C11. \end{aligned} \tag{28}$$

4. Virtual Resource Allocation with PNC Aided Self-backhaul

Since $\boldsymbol{X}$ is binary integer variable, problem $P1$ is combinatorial and discrete. Moreover, due to the expression of F_{MVNO} and constraint $C1$, $P1$ is also non-convex. Thus, the computational complexity of the problem is high. In this section, we decompose the problem into two sub problems and develop a two-phase iteration algorithm for problem $P1$. In sub section 4.1, iteration process I is presented, in which we solve X, Y, and Z with fixed a and P. And then, sub section 4.2 presents iteration process II to solve a and P when X, Y, and Z are given. Finally, the whole solution for the proposed virtual resource allocation is presented accordingly.

4.1 Iteration Process I

To reduce the computational complexity, we firstly assume that the spectrum indicator $\boldsymbol{a}$ are given, so problem $P1$ is reduced to the following problem.

$$\begin{aligned} P2: \quad & \max_{\boldsymbol{X},\boldsymbol{Y},\boldsymbol{Z},\boldsymbol{P},\boldsymbol{P}_m} \sum_{i=1}^{N}\{\sum_{m=1}^{M}(\sum_{u\in\boldsymbol{U}_i}\delta_u C_u^m(\boldsymbol{X},\boldsymbol{Y},\boldsymbol{Z},\boldsymbol{P},\boldsymbol{P}_m)-\gamma_m T_i^m(\boldsymbol{X},\boldsymbol{Y},\boldsymbol{Z},\boldsymbol{P},\boldsymbol{P}_m) \\ & \qquad\qquad -Q_i^m(\boldsymbol{X},\boldsymbol{Y},\boldsymbol{Z},\boldsymbol{P},\boldsymbol{P}_m))\} \\ & s.t. \ \ C1 \sim C9, C11. \end{aligned} \tag{29}$$

Remark 1: If problem $P2$ is feasible, the optimal solution is achieved only when $x_u^{m,0}y_u^{m,0} \neq 0$.

□

We obtain **Remark 1** through a contradiction statement. Firstly, it is assumed that the optimal solution $(\boldsymbol{X}^*,\boldsymbol{Y}^*,\boldsymbol{Z}^*,\boldsymbol{a}^*,\boldsymbol{P}^*,\boldsymbol{P}_m^*)$ of $P1$ is obtained for problem $P2$ when $\sum_{u\in\boldsymbol{U}_i} x_u^{m,0}y_u^{m,0}=0$. Since $x\in\{0,1\}$, $y\in(0,1)$, it can be deduced that $x_u^{m,0}y_u^{m,0}=0, \forall u\in\boldsymbol{U}_i$. Thus, the objective function can be written as

$$\begin{aligned} F_{MVNO} = & \sum_{i=1}^{N}\{\sum_{m=1}^{M}(\sum_{u\in\boldsymbol{U}_i}\delta_u \sum_{j\in\boldsymbol{S}_m} x_u^{m,j}y_u^{m,j}R_u^{m,j} \\ & -\gamma_m(w_m \sum_{j\in\boldsymbol{S}_m \& u\in\boldsymbol{U}_i} x_u^{m,j}y_u^{m,j}(1-a_m)B_m P) \\ & -\sum_{j\in\boldsymbol{S}_m}(1-a_m)Pz_m^{Sj}\sum_{u\in\boldsymbol{U}_i\&\boldsymbol{U}_m^{Sj}} x_u^{m,j}y_u^{m,j}R_u^{m,j})\}. \end{aligned} \tag{30}$$

Since $x_u^{m,0}y_u^{m,0}=0$, it indicates that no users are associated with the MBS, so we assume that $\boldsymbol{a}^*=0$, which means no spectrum are allocated to $u_i, u_i\in\boldsymbol{U}_m$. Then we set $\boldsymbol{a}^+=\boldsymbol{a}^*+\Delta$,

$\Delta > 0$, and substitute it into (30), it is obvious that $F_{MVNO}(\boldsymbol{a}^{+}) > F_{MVNO}(\boldsymbol{a}^{*})$ because there are

$$\left.\frac{\partial F_{MVNO}}{\partial \boldsymbol{a}^{*}}\right|_{\boldsymbol{a}^{*}=0} = \sum_{i=1}^{N}\{\sum_{m=1}^{M}(\sum_{u\in \boldsymbol{U}_i}\delta_u(2Pz_m^{Sj}-1)\sum_{j\in \boldsymbol{S}_m}x_u^{m,j}y_u^{m,j}B_m\log(1+\frac{P|h_m^{Sj}|^2}{(1+\frac{1}{|h_{Sj}^{u}|^2})\sigma^2})$$
$$+\gamma_m(w_m\sum_{j\in \boldsymbol{S}_m \& u\in \boldsymbol{U}_i}x_u^{m,j}y_u^{m,j}B_mP))\} > 0. \quad (31)$$

This result is contradicted with the assumption that $\boldsymbol{a}^{*}$ is the optimal value. Therefore, $\boldsymbol{a}^{*} \neq 0$, which means that there exist free spectrum for the MBS to access the users. So on the basis of the optimal solution, we utilize this free spectrum to access one more user through the MBS, and $x_0^{+}y_0^{+}$ are the indicator associated to this user. Thus, the gap of the objective function between new parameters and the optimal solution can be expressed as

$$\begin{aligned} &F_{MVNO}(x_0^{+},y_0^{+},\boldsymbol{X}^{*},\boldsymbol{Y}^{*},\boldsymbol{Z}^{*},\boldsymbol{a}^{*},\boldsymbol{P}^{*},\boldsymbol{P}_m^{*})-F_{MVNO}(\boldsymbol{X}^{*},\boldsymbol{Y}^{*},\boldsymbol{Z}^{*},\boldsymbol{a}^{*},\boldsymbol{P}^{*},\boldsymbol{P}_m^{*}) \\ &=\sum_{i=1}^{N}\{\sum_{m=1}^{M}(\sum_{u\in \boldsymbol{U}_i}x_0^{+}y_0^{+}(\delta_uR_u^{m,0}(a_m^{*})-\gamma_m a_m^{*}B_mP_m))\}. \end{aligned} \quad (32)$$

Since $\delta_u >> \gamma_m$ [15] in practice, it can be deduced that (32) > 0. In other word, the solution $(x_0^{+},y_0^{+},\boldsymbol{X}^{*}, \boldsymbol{Y}^{*},\boldsymbol{Z}^{*},\boldsymbol{a}^{*},\boldsymbol{P}^{*},\boldsymbol{P}_m^{*})$ increases the value of the objective function, which is contradicted with the assumption that $(\boldsymbol{X}^{*},\boldsymbol{Y}^{*},\boldsymbol{Z}^{*},\boldsymbol{a}^{*},\boldsymbol{P}^{*},\boldsymbol{P}_m^{*})$ is the optimal solution. Therefore, **Remark 1** is obtained.

On the basis of **Remark 1**, we can derive the folowing remark, so as to reduce the variables of problem $P2$.

Remark 2: For problem $P2$, if the optimal solution exists, the objective function in (29) achieves the maximum value only when $P+P_m=P_m^{T}$ holds.

Firstly, we assume that the optimal solution is feasible for problem $P2$ when $P^{*}+P_m^{*}<P_m^{T}$, in which P^{*} and P_m^{*} are the corresponding elements of the optimal solution. The derivation of the objective function F_{MVNO} respect to P_m can be expressed as

$$\frac{\partial F_{MVNO}}{\partial P_m}=\sum_{i=1}^{N}\{\sum_{m=1}^{M}(\sum_{u\in \boldsymbol{U}_i}\delta_u x_u^{m,0}y_u^{m,0}\frac{a_mB_m}{\ln 2(1+\frac{P_m|h_u^{m}|^2}{\sigma^2})}-\gamma_m\sum_{u\in \boldsymbol{U}_i \& u\in \boldsymbol{U}_m}x_u^{m,0}y_u^{m,0}a_mB_m)\}. \quad (33)$$

With the inequality $P_m<P_m^{T}$, (33) can be bounded as

$$\frac{\partial F_{MVNO}}{\partial P_m}>\sum_{i=1}^{N}\{\sum_{m=1}^{M}(\sum_{u\in \boldsymbol{U}_i \& u\in \boldsymbol{U}_m}x_u^{m,0}y_u^{m,0}a_mB_m(\frac{\delta_u}{\ln 2(1+\frac{P_m^{T}|h_u^{m}|^2}{\sigma^2})}-\gamma_m))\}. \quad (34)$$

According to **Remark 1**, there is $x_u^{m,0}y_u^{m,0}\neq 0$, coupled with $\delta_u >> \gamma_m$, it can be deduced that (34) > 0, in other word, there is $F_{MVNO}(P_m^{*}+P_\Delta,P^{*})>F_{MVNO}(P_m^{*},P^{*})$ when $P_\Delta>0$. Since

$P^* + P_m^* < P_m^T$, there always exists a certain $P_\Delta > 0$ which satisfies $P^* + P_m^* + P_\Delta < P_m^T$. Hence, the value of F_{MVNO} can be increased by replacing P_m^* with $P_m^* + P_\Delta$, which is contradicted with the assumption that P_m^* is the element of the optimal solution. Thus, **Remark 2** is obtained.

With **Remark 2**, we utilize $P_m = P_m^T - P$ to simplify problem $P2$, so the variable P_m in (29) can be eliminated. Next, by substituting (7) and (25) into (17), constraint $C1$ can be rewritten as

$$\log(1+\frac{P\,|h_m^{Sj}|^2}{(1+\frac{1}{|h_u^{Sj}|^2})\sigma^2}) \le \log(1+\frac{P\,|h_m^{Sj}|^2}{\sigma^2}). \tag{35}$$

It is obvious that the above inequality holds, which indicates that when C9 holds, C1 is invalid and can be eliminated.

To transfer problem $P2$ into the convex problem, we employ (25) to eminate variable $\boldsymbol{Z}$, so z_m^{Sj} is replaced by $\sum x_u^{m,j} y_u^{m,j}$ in (29). Then we assume that the transmission power P is also given. Besides, we relax $x_u^{m,j}$ to be real variables so that $0 \le x_u^{m,j} \le 1$. Also, (17) is utilized to approximate $\sum x_u^{m,j} y_u^{m,j} R_u^{m,j}$, so the objective function is simplified as

$$\begin{aligned} F_{MVNO} \approx \sum_{i=1}^{N}\{\sum_{m=1}^{M}(\sum_{u\in\boldsymbol{U}_i}\delta_u(x_u^{m,0}y_u^{m,0}a_m B_m\log(1+\frac{(P_m^T-P)\,|h_u^m|^2}{\sigma^2}) \\ +\sum_{j\in\boldsymbol{S}_m} x_u^{m,j}y_u^{m,j}(1\text{-}a_m)\; B_m\log(1+\frac{P\,|h_m^{Sj}|^2}{\sigma^2}) \\ -\gamma_m(\sum_{u\in\boldsymbol{U}_m\&u\in\boldsymbol{U}_i} x_u^{m,0}y_u^{m,0}a_m B_m(P_m^T-P)+w_m\sum_{j\in\boldsymbol{S}_m\&u\in\boldsymbol{U}_i} x_u^{m,j}y_u^{m,j}(1-a_m)B_m P) \\ -\sum_{j\in\boldsymbol{S}_m}(1-a_m)^2 PB_m(\sum_{u\in\boldsymbol{U}_i\&\boldsymbol{U}_m^{Sj}} x_u^{m,j}y_u^{m,j})^2\log(1+\frac{P\,|h_m^{Sj}|^2}{\sigma^2}))\}. \end{aligned} \tag{36}$$

We then define $\theta_u^{m,0} = x_u^{m,0} y_u^{m,0}, \lambda_u^{m,j} = x_u^{m,j} y_u^{m,j}$ and substitute them into (36), so problem $P2$ can be reduced to the following problem:

$$\begin{aligned} P3: \quad & \max_{\boldsymbol{\theta},\boldsymbol{\lambda}} \sum_{i=1}^{N}\{\sum_{m=1}^{M}(C'_{u,m}+T'_{i,m}+Q'_{i,m})\} \\ s.\,t.\quad & C'1: \quad 0 \le \theta_u^{m,0} \le 1. \\ & C'2: \quad \sum_{u\in\boldsymbol{U}_m}\theta_u^{m,0} \le 1, \forall m. \\ & C'3: \quad 0 \le \lambda_u^{m,j} \le 1, \forall m, j. \\ & C'4: \quad \sum_{u\in\boldsymbol{U}_m^{Sj}}\lambda_u^{m,j} \le 1, \forall m, j. \\ & C'5: \quad \theta_u^{m,0}+\lambda_u^{m,j} \le 1, \forall m, j. \end{aligned} \tag{37}$$

in which

$$C'_{u,m}=\sum_{u\in \boldsymbol{U}_i}\delta_u\theta_u^{m,0}a_mB_m\log(1+\frac{(P_m^T-P)|h_u^m|^2}{\sigma^2})+\sum_{j\in \boldsymbol{S}_m}\lambda_u^{m,j}(1\text{-}a_m)\ B_m\log(1+\frac{P|h_m^{Sj}|^2}{\sigma^2}), \tag{38}$$

$$T'_{i,m}=-\gamma_m(\sum_{u\in \boldsymbol{U}_m \& u\in \boldsymbol{U}_i}\theta_u^{m,0}a_mB_m(P_m^T-P)+w_m\sum_{j\in \boldsymbol{S}_m}\lambda_u^{m,j}(1-a_m)B_mP), \tag{39}$$

$$Q'_{i,m}=-\sum_{j\in \boldsymbol{S}_m}(1-a_m)^2PB_m(\sum_{u\in \boldsymbol{U}_i \& \boldsymbol{U}_m^{Sj}}\lambda_u^{m,j})^2\log(1+\frac{P|h_m^{Sj}|^2}{\sigma^2}). \tag{40}$$

The convexity of problem $P3$ is proved through the following theorem.

Theorem 1: If problem $P3$ is feasible, it is jointly convex with respect to all optimization variables $\theta_u^{m,0}$ and $\lambda_u^{m,j}$.

Proof : The proof is provided in **Appendix A**.

Due to the convexity of problem $P3$, many solutions can be employed to solve it. Here, the steepest descent method is utilized to obtain the optimal solution $(\theta_u^{m,0})^*$ and $(\lambda_u^{m,j})^*$ for prolem $P3$. Next, to recover the discrete value of $\boldsymbol{X}^*$, the marginal benefit method [24] is utilized. We denote F'_{MVNO} as the objective function in (37), so the indicator $(x_u^{m,j})^*$ can be recovered as

$$(x_u^{m,0})^*=\begin{cases}1 \text{ if } (\theta_u^{m,0})^*=\max\limits_{m,j}\{\frac{\partial F'_{MVNO}}{\partial\theta_u^{m,0}},\frac{\partial F'_{MVNO}}{\partial\lambda_u^{m,j}}\} \ \&\&\ \frac{\partial F'_{MVNO}}{\partial\theta_u^{m,0}}\geq 0\\ 0 \text{ otherwise}\end{cases}. \tag{41}$$

$$(x_u^{m,j})^*=\begin{cases}1 \text{ if } (\lambda_u^{m,j})^*=\max\limits_{m,j}\{\frac{\partial F'_{MVNO}}{\partial\theta_u^{m,0}},\frac{\partial F'_{MVNO}}{\partial\lambda_u^{m,j}}\} \ \&\&\ \frac{\partial F'_{MVNO}}{\partial\lambda_u^{m,j}}\geq 0\\ 0 \text{ otherwise}\end{cases}. \tag{42}$$

Hence, $\boldsymbol{X}^*$ are obtained. After that, $(y_u^{m,j})^*$ can be recovered by solving problem (36) coupled with constraints $C4\sim C6$, which is convex respect to $y_u^{m,j}$ with the known $(x_u^{m,j})^*$. When $\boldsymbol{X}^*$ and $\boldsymbol{Y}^*$ are solved, $\boldsymbol{Z}^*$ can be also recovered through (25). Thus, $\boldsymbol{X}$,$\boldsymbol{Y}$ and $\boldsymbol{Z}$ are obtained under fixed spectrum indicator $\boldsymbol{a}$ and power $\boldsymbol{P}$.

4.2 Iteration Process II

When $\boldsymbol{X}$, $\boldsymbol{Y}$, and $\boldsymbol{Z}$ are obtained, the original problem $P1$ will be reduced as following:

$$\begin{aligned} P4: \quad & \max_{\boldsymbol{P},\boldsymbol{a}}\sum_{i=1}^{N}\{\sum_{m=1}^{M}(C''_{u,m}+T''_{i,m}+Q''_{i,m})\} \\ & s.\,t. \qquad C10\sim C11. \end{aligned} \tag{43}$$

in which $C''_{u,m}$, $T''_{i,m}$ and $Q''_{i,m}$ are defined as

$$C''_{u,m} = \sum_{u\in \boldsymbol{U}_i} \delta_u D_u^{m,0} a_m B_m \log(1+\frac{(P_m^T - P)\,|\,h_u^m\,|^2}{\sigma^2}) + \sum_{j\in \boldsymbol{S}_m} D_u^{m,j} (1\text{-}a_m)\ B_m \log(1+\frac{P\,|\,h_m^{Sj}\,|^2}{(1+\frac{1}{|h_{Sj}^u|^2})\sigma^2}), \tag{44}$$

$$T''_{i,m} = -\gamma_m (\sum_{u\in \boldsymbol{U}_m \& u\in \boldsymbol{U}_i} D_u^{m,0} a_m B_m (P_m^T - P) + w_m \sum_{j\in \boldsymbol{S}_m} D_u^{m,j} (1-a_m) B_m P), \tag{45}$$

$$Q''_{i,m} = -\sum_{j\in \boldsymbol{S}_m} (1-a_m)^2 P B_m (\sum_{u\in \boldsymbol{U}_i \& \boldsymbol{U}_m^{Sj}} D_u^{m,j})^2 \log(1+\frac{P\,|\,h_m^{Sj}\,|^2}{(1+\frac{1}{|h_{Sj}^u|^2})\sigma^2}). \tag{46}$$

while $D_u^{m,0}$ and $D_u^{m,j}$ are constants when $\boldsymbol{X}$ and $\boldsymbol{Y}$ are given. Here we propose a theorem to solve problem $P4$.

Theorem 2: If problem $P4$ is feasible, it is jointly convex with respect to the variables $\boldsymbol{P}$ and $\boldsymbol{a}$.

Proof : The proof is presented in **Appendix B**.

Since $P4$ is a convex problem, we utilize the steepest descent method [23] to obtain the optimal solution a_m^* and P^*. After that, a_m^* and P^* can be substituted into (37) to start a new iteration, which yields new values to update $\boldsymbol{X}^*, \boldsymbol{Y}^*$ and $\boldsymbol{Z}^*$. We employ the utility of MVNOs as the stop criterion, that is, the whole iteration process stops if the growth of the utility is less than the threshold. Hence, when the iteration stops, the approximate solution of $P1$ as well as the corresponding virtual resource allocation is obtained. The iteration process is presented as Algorithm 1.

Algorithm 1 PNC aided virtual resource allocation with self-backhaul

Step 1: Initiatize $a_m^O = 0.5, P^O = 0.5P_m^T, F_{MVNO}^O = 0, O = 0, \chi^T$.

Step 2: Input $\boldsymbol{a}^O, \boldsymbol{P}^O$.

Solve problem $P3$ in (37) by the steepest method.

Output $\boldsymbol{\theta}^*, \boldsymbol{\lambda}^*$.

Step 3: Recover $\boldsymbol{X}^{O+1}, \boldsymbol{Y}^{O+1}$ and $\boldsymbol{Z}^{O+1}$ by utilizing $\boldsymbol{\theta}^*, \boldsymbol{\lambda}^*$ and (41) to (42).

Step 4: Input $\boldsymbol{X}^{O+1}, \boldsymbol{Y}^{O+1}$ and $\boldsymbol{Z}^{O+1}$ into (43) and solve problem $P4$

Output a_m^{O+1}, P^{O+1}.

Step 5: Input $\boldsymbol{X}^{O+1}, \boldsymbol{Y}^{O+1}, \boldsymbol{Z}^{O+1}, a_m^{O+1}$ and P^{O+1} into (16) and calculate F_{MVNO}^{O+1}

Step 6: While $\| F_{MVNO}^{O+1} - F_{MVNO}^{O} \| > \chi^T$

$O = O + 1$.

Go to Step 2.

End while

Step 7: Output the solution $\boldsymbol{X}^O, \boldsymbol{Y}^O, \boldsymbol{Z}^O, \boldsymbol{a}^O$ and $\boldsymbol{P}^O$.

5. Simulation Results

In this section, the developed algorithm is examined through simulations, in which the scheme in [15] and the one without virtualization and self-backhaul [25] are compared as the benchmark. In order to guarantee the fairness during the comparison, the method in [25] is adopted to normalize the utility of MVNOs for all the compared algorithms. As the performance metrics, the utilities of MVNOs, users, InPs and the resource utilization ratio are simulated to evaluate the network resource utilization. In the simulations, M=N=2, that is, a square area is covered by two InPs, in which two MVNOs lease network resources from the InPs and provide access service to the users in the area. Each InP owns one MBS and four SBSs. The MBS locates at the center of the area, while the SBSs and the users are randomly deployed. Besides, the spectrum bandwidth $B_m = 10$ M Hz, and the power budget $P_m^T = 46.0109$ dB [15]. For each user, $\delta_u = 10^6$ and $w_m = 10^{-3}$, while the deliberated price $\gamma_m = 5$ between all the InPs and MVNOs. In the iteration process of the proposed algorithm, the stop threshold $\chi_T = 100$.

Fig. 3 depicts the utility of MVNOs with respect to the number of users. For all the compared schemes, it shows that the growth of users increase the utility of MVNOs, while the proposed algorithm and benchmark [15] are obviously superior to the one in [25]. This behavior is acounted for two factors, on the one hand, virtualization enables optimal matching between the users and the channels, which can improve the profits of the MVNOs and InPs, on the other hand, wireless self-backhauls reduce the expense of backhauls significantly compared with conventional method. Considering all these two factors, it indicates that virtualization and wireless self-backhauls are constructive for the utility of the networks. Besides, the proposed algorithm outperforms the one in [15], and when the number of users is small, the performances of the two algorithms are close, while the gap expands with the growth of the users. This is because the proposed algorithm deals with the residual interference through PNC. Meanwhile, due to TS separation, it also suffers no interference from other SBSs, so the expense of backhauls can be reduced. When the number of users is small, the residual interference and the interference from other SBSs are light, so the advantage of the proposed algorithm is not obvious. As the user number grows, these interferences will rise, and it becomes more and more considerable to reduce the interferences through the proposed PNC aided self-backhaul.

The average utilities of the users for the compared schemes are shown in **Fig. 4**. It can be observed that as the number of users grows, the average utility of individual user is declining. This is because the total network resource is limited, so the resource allocated to a certain user becomes less when more and more users are accessed into the network. The proposed algorithm and [15] outperform the one in [25], because from perspective of the users, they can get network resource more flexibly, so there are more chances to access with superior wireless channels, which will increase the achievable rate of the users. Besides, self-backhauls also help to reduce the expense of backhauls. Compared with the one in [15], the proposed algorithm enables the users to obtain more profits, because the expenses and the interference are reduced through PNC aided self-backhaul. In addition, as the number of users increases, the performance gap decreases, which is caused by the channel unbalance of PNC scheme [20]. According to (7), it can be seen that PNC can supply favorable achievable rate only when h_m^{Sj} and h_{Sj}^u are in good state, so when more users are accessed, the users with bad channels also increase, which decrease the constructive effect of PNC and the achievable rate of the users.

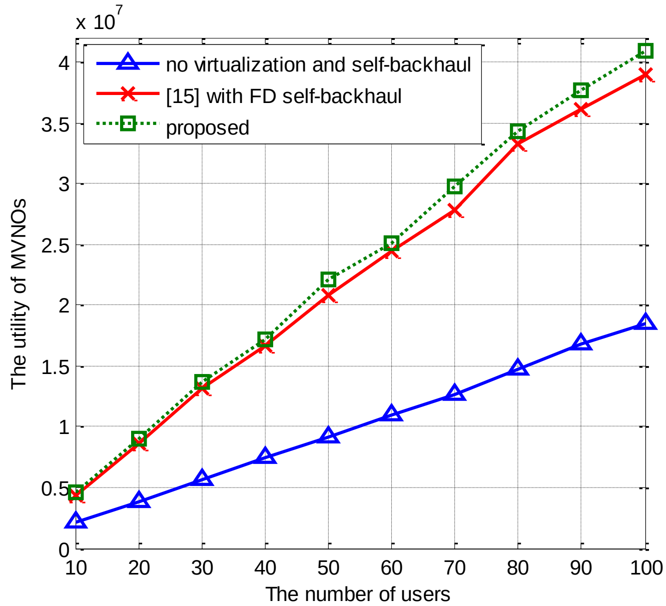

Fig. 3. The utility of MVNO.

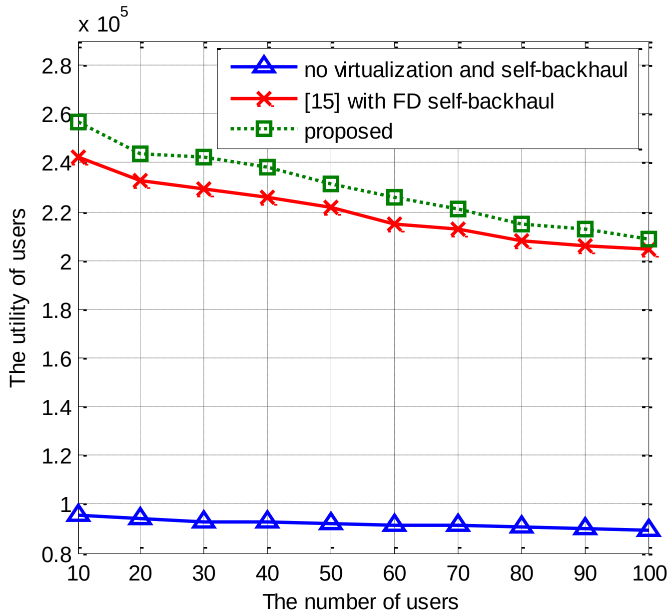

Fig. 4. The utility of users.

Fig. 5 shows the utility of InPs with respect to the number of users. In general, for the compared algorithms, the utility increases at first and then tends to be flat with the growth of the users. The reason is that when more and more users are accessed, it increases the demand for the network resource, so InPs will get more incomes from MVNOs through network resource leasing. On the other hand, it is harmful for the MVNOs to lease all the network resources, because the expense may be beyond the incomes. Hence, with the compared algorithms, only appropriate amount resource will be allocated. By benefiting from virtualization and self-backhaul, the proposed algorithm and [15] are superior to the one in [25]. Similarly, since the proposed PNC scheme reduces the expense of self-backhaul and interference, it outperforms [15]. As shown in **Fig. 5**, the gap becomes obvious when the number of users is large, because in that case, more users will be allocated to the SBSs, so the advantage of PNC aided self-backhaul is apparent.

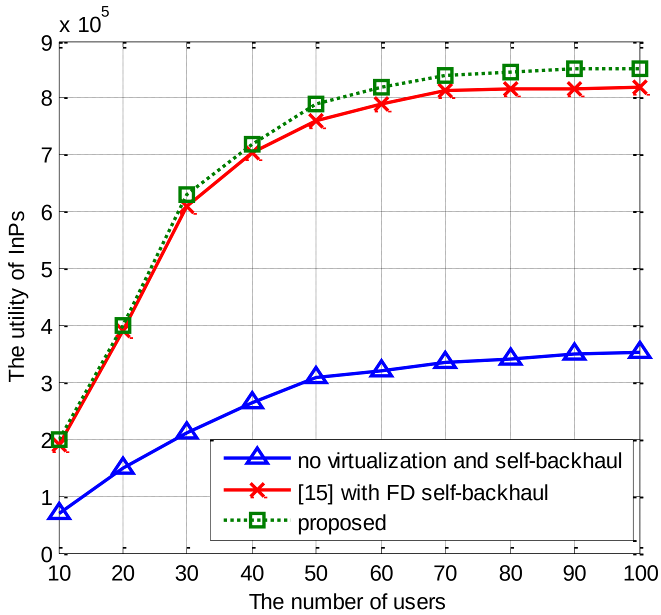

Fig. 5. The utility of InPs.

Fig. 6 depicts the resource utilization ratio of the network with respect to the number of users. Similarly, for all the compared algorithms, the resource utilization ratio increases with the growth of the users and trends to be flat when the number of users is large. In fact, as the number of users grows, more users will be allocated to SBSs, which are all in heavy load and have less extra TS resource for the subsequent users. Also, the subsequent users will not be allocated to MBS because of the high expense either, which makes the resource utilization ratio flat. It can be seen that the proposed algorithm consumes more resources than the other two, because in our scheme, the PNC aided self-backhaul will attracts more users to be associated for its low cost, so more SBSs will be consumed. Besides, in the proposed PNC scheme, to reduce the interference between the SBSs, each SBS is separated from each other through TS, so more TS resource of SBS will be consumed compared with [15]. Combined with the results in **Figs. 3**, **4** and **5**, it can be summarized that although the proposed algorithm consumes more resources, it yields optimal utility of the MVNOs, InPs and users, so the construction effect of PNC to the utility efficiency of the virtual network resource is verified.

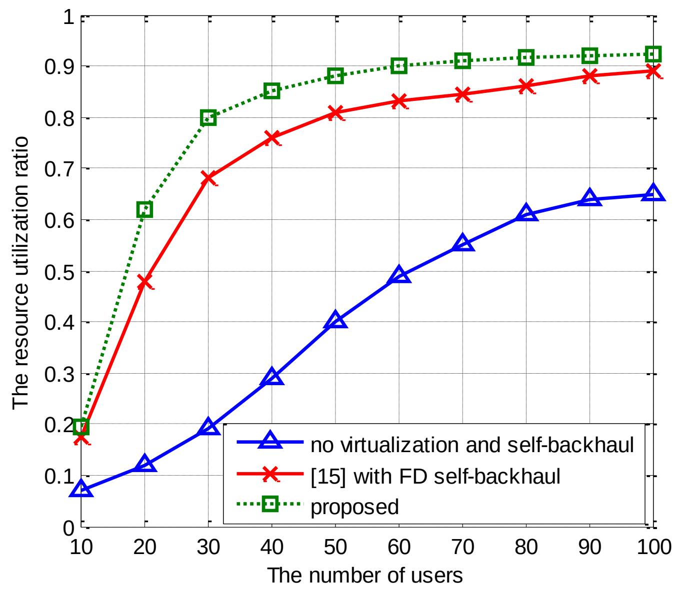

Fig. 6. The resource utilization ratio.

6. Conclusions

In this paper, we have proposed a PNC aided self-backhaul to mitigate the destructive effects of the residual self-interference in the virtualized small cell networks. We have formulated a mixed combinatorial optimization problem to maximize the total utility of MVNOs with the proposed scheme. And to solve the problem efficiently, a two-phase iteration algorithm has been developed. Simulations demonstrated that the proposed scheme is able to make full use of the PNC to reduce the residual interference, and improve the profits of MVNOs, InPs and users effectively. Besides, the construction effect of PNC to the utility efficiency of the virtual network resource was also verified. In the future, we will further investigate the PNC aided self-backhaul and virtual resource allocation when the users are equipped with multi-antenna.

Appendix A

Proof of Theorem 1

Proof : Since the constraints $C'1, C'2, C'3, C'4, C'5$ are linear, they are obviously convex, which indicates that the feasible set is convex. Next, it can be observed that the objective function in (37) is the linear sum of $C'_{u,m}, T'_{i,m}$, and $Q'_{i,m}$. For $C'_{u,m}(\theta_u^{m,0})$ and $T'_{i,m}(\theta_u^{m,0})$, they are both the linear functions with respect to $\theta_u^{m,0}$, while $Q'_{i,m}$ is not correlate with $\theta_u^{m,0}$. Therefore, the convexity of the objective function with respect to $\theta_u^{m,0}$ is proved, because the linear sum of convex function is still convex [23]. Similarly, for the variable $\lambda_u^{m,j}$, $C'_{u,m}(\lambda_u^{m,j})$ and $T'_{i,m}(\lambda_u^{m,j})$ are still linear functions. Note that $Q'_{i,m}(\lambda_u^{m,j})$ is the sum of quadratic function with respect to $(\lambda_u^{m,j})^2$. Since $\frac{\partial^2 Q'_{i,m}}{\partial(\lambda_u^{m,j})^2} \geq 0$, it can be deduced that $Q'_{i,m}(\lambda_u^{m,j})$ is a concave function with respect to $\lambda_u^{m,j}$. According to the fact that a negative concave function is convex, the convexity of $-\sum Q'_{i,m}$ is also proved. Thus, it is derived that the objective function in $P3$ is convex, for it is the sum of convex functions. Coupled with the convex feasible set, the convexity of problem $P3$ is proved.

Appendix B

Proof of Theorem 2

Proof : It is obvious that $C10$ and $C11$ are linear, so the feasible set is convex. We denote F''_{MVNO} as the objective function in (43), and it is easy to obtain $\frac{\partial^2 F''_{MVNO}}{\partial(a_m)^2} < 0$, so F''_{MVNO} is convex with respect to a. For the variable P, F''_{MVNO} is the sum of $C''_{u,m}(P), T''_{i,m}(P)$ and $Q''_{i,m}(P)$. It can be derived that

$$\frac{\partial^2 C''_{u,m}}{\partial P^2} = \sum_{i=1}^{N}\{\sum_{m=1}^{M}(\sum_{u\in \boldsymbol{U}_i} -\frac{D_u^{m,0} a_m B_m}{(1+\frac{(P_T-P)|h_u^{m,0}|^2}{\sigma^2})^2} - \sum_{j\in \boldsymbol{S}_m} \frac{(1-a_m)D_u^{m,j}B_m}{(1+\frac{P|h_m^{Sj}|^2}{(1+\frac{1}{|h_{Sj}^u|^2})\sigma^2})^2})\} < 0, \tag{47}$$

so $C''_{u,m}(P)$ is convex with respect to P. Also, it is easy to know that $T''_{i,m}(P)$ is convex, since it is the linear function of P. For the function $Q''_{i,m}(P)$, the second order derivation can be obtained as

$$\frac{\partial^2 Q''_{i,m}}{\partial P^2} = \sum_{i=1}^{N}\{\sum_{m=1}^{M}(\sum_{u\in \boldsymbol{U}_i} \frac{(1-a_m)^2 B_m(\sum_{u\in \boldsymbol{U}_m^{Sj}} D_u^{m,j})^2}{1+\frac{P|h_m^{Sj}|^2}{(1+\frac{1}{|h_{Sj}^u|^2})\sigma^2}})\} > 0, \tag{48}$$

and it can be derived that $-Q''_{i,m}(P)$ is convex with respect to P. Hence, it is deduced that F''_{MVNO} is the sum of convex functions with respect to P, and the convexity of problem $P4$ is proved.

References

[1] C. Liang and F. Richard Yu, "Wireless network virtualization: a survey, some research issues and challenges," *IEEE Communications Surveys and Tutorials*, vol. 17, no. 1, pp. 358-380, Firstquarter, 2015. Article (CrossRef Link).

[2] F. Fu and U. Kozat, "Stochastic game for wireless network virtualization," *IEEE/ACM Transactions on Networking*, vol. 21, no. 1, pp. 84-97, Feb. 2013. Article (CrossRef Link).

[3] C. Xavier, J. Swetina, T. Guo, et al, "Radio access network virtualization for future mobile carrier networks," *IEEE Communications Magazine*, vol. 51, no. 7, pp. 27-35, July, 2013. Article (CrossRef Link).

[4] Y. Zaki, L. Zhao, C. Goerg and A. Timm-Giel, "LTE wireless virtualization and spectrum management," in *Proc. of 2010 Joint IFIP Wireless and Mobile Networking Conference*, pp. 1-6, Oct. 2010. Article (CrossRef Link).
[5] A. Moubayed, A. Shami and H. Lutfiyya, "Wireless resource virtualization with device-to-device communication underlaying LTE network," *IEEE Transactions on Broadcasting*, pp. 734–740, November, 2015. Article (CrossRef Link).
[6] R. Kokku, R. Mahindra, H. Zhang, and S. Rangarajan, "NVS: A substrate for virtualizing wireless resources in cellular networks," *IEEE/ACM Transactions on Networking*, vol. 20, no. 5, pp. 1333–1346, Oct. 2012. Article (CrossRef Link).
[7] A. Tzanakaki, M. P. Anastasopoulos, G. Zervas, et al, "Virtualization of heterogeneous wireless-optical network and IT infrastructures in support of cloud and mobile cloud services," *IEEE Communications Magazine*, vol. 51, no. 8, pp. 155-161, August, 2013. Article (CrossRef Link).
[8] G. Bhanage, D. Vete, I. Seskar, and D. Raychaudhuri, "SplitAP: Leveraging wireless network virtualization for flexible sharing of WLANs," in *Proc. of IEEE Globecom*, pp. 1–6, January, 2011. Article (CrossRef Link).
[9] J. Hoydis, M. Kobayashi and M. Debbah, "Green small cell networks," *IEEE Vehicular Technology Magazine*, vol. 6, no. 1, pp. 37-43, March, 2011. Article (CrossRef Link).
[10] M. Jo, T. Maksymyuk, R. L. Batista, et al., "A survey of converging solutions for heterogeneous mobile networks," *IEEE Wireless Communications*, vol. 21, no. 6, pp. 54-62, December, 2014. Article (CrossRef Link).
[11] J. G. Andrews, H. Claussen, M. Dohler, S. Rangan, and M. C. Reed, "Femtocells: past, present, and future," *IEEE Journal on Selected Areas in Communications*, vol. 30, no. 3, pp. 497–508, March, 2012. Article (CrossRef Link).
[12] D. Chen, T. Quek and M. Kountouris, "Backhauling in heterogeneous cellular networks: modeling and tradeoffs," *IEEE Transactions on Wireless Communications*, vol. 14, no. 6, pp. 3194-3206, February, 2015. Article (CrossRef Link).
[13] O. Tipmongkolsilp, S. Zaghloul and A. Jukan, "The evolution of cellular backhaul technologies: current issues and future trends," *IEEE Communications Surveys and Tutorials*, vol. 13, no. 1, pp. 97-113, May, 2011. Article (CrossRef Link).
[14] X. Ge, H. Cheng, M. Guizani and T. Han, "5G wireless backhaul networks: challenges and research advances," *IEEE Network*, vol. 28, no. 6, pp. 6-11, November, 2014. Article (CrossRef Link).
[15] L. Chen, F. R. Yu, H. Ji, et al, "Distributed virtual resource allocation in small cell networks with full duplex self-backhauls and virtualization," *IEEE Transactions on Vehicular Technology*, August, 2015. Article (CrossRef Link).
[16] A. Sabharwal, P. Schniter, D. Guo, et al, "In-band full-duplex wireless: challenges and opportunities," *IEEE Journal on Selected Areas in Communications*, vol. 32, no. 9, pp. 1637-1652, June, 2014. Article (CrossRef Link).
[17] R. Ahlswede, C. Ning, S. Li, and R. Yeung, "Network information flow," *IEEE Transactions on Information Theory*, vol. 46, no. 12, pp. 1204-1216, Jul 2000. Article (CrossRef Link).
[18] H. Q. Lai and K. J. R. Liu, "Space-time network coding," *IEEE Transactions on Signal Processing*, vol. 59, no. 4, pp. 1706–1718, April, 2011. Article (CrossRef Link).
[19] K. Xiong, P. Y. Fan, H. C. Yang, and K. B. Letaief, "Space-time network coding with overhearing relays," *IEEE Transactions on Wireless Communications*, vol. 13, no. 7, pp. 3567–3582, July, 2014. Article (CrossRef Link).
[20] Y. Zhang, K. Xiong, F. P. Fan, X. F. DI and X. W. Zhou, "Outage performance of space-time network coding with overhearing AF relays," *IEEE Communications Letters*, vol. 19, no. 12, pp. 2234-2237, Dec. 2015. Article (CrossRef Link).
[21] S. Zhang, S. Liew, and P. Lam, "Hot topic: Physical layer network coding" in *Proc. of ACM International Conference on Mobile Computing and Networking*, pp. 358-36, September, 2006. Article (CrossRef Link).

[22] M. Jo, T. Maksymyuk, B. Strykhalyuk, C. Cho, "Device-to-device-based heterogeneous radio access network architecture for mobile cloud computing," *IEEE Wireless Communications*, vol. 22, no. 3, pp. 50-58, June, 2015. Article (CrossRef Link).
[23] S. Boyd and L. Vandenberghe, "Convex Optimization," *Cambridge University Press*, 2009. Article (CrossRef Link).
[24] C. Y. Wong, R. S. Cheng, K. B. Letaief, and R. D. Murch, "Multiuser OFDM with adaptive subcarrier, bit, and power allocation," *IEEE Journal on Selected Areas in Communications*, vol. 17, no. 10, pp. 1747–1758, Oct. 1999. Article (CrossRef Link).
[25] Q. Ye, B. Rong, Y. Chen, et al, "User association for load balancing in heterogeneous cellular networks," *IEEE Transactions on Wireless Communications*, vol. 12, no. 6, pp. 2706–2716, June, 2013. Article (CrossRef Link).

Yulun Cheng received his Ph. D. degree from Jiangsu Key Lab of Wireless Communications, Nanjing University of Posts and Telecommunications (NUPT), China, in 2014. He is currently working as a lecturer with college of Telecommunications & Information Engineering, NUPT. His current research interests include wireless virtual networks, network coding, and NFV mapping.

Longxiang Yang is with the College of Communications and Information Engineering, Nanjing University of Posts and Telecommunications (NUPT), Nanjing, China. He is a full professor and a doctoral supervisor with NUPT. He has fulfilled multiple National Natural Science Foundation projects of China. He has authored and coauthored more than 100 technical papers published in various journals and conferences. His research interests include cooperative communication and network coding, wireless communication theories, key technologies of mobile communication systems, ubiquitous networks, and Internet of things.

Hongbo Zhu received the B.S. degree in communications engineering from the Nanjing University of Posts and Telecommunications, Nanjing, China, and the Ph. D. degree in information and communications engineering from Beijing University of Posts and Telecommunications, Beijing, China, in 1982 and 1996, respectively. He is presently working as a professor and vice-president with Nanjing University of Posts and Telecommunications, Nanjing, China. He is also the Head of the Coordination Innovative Center, IoT Technology and Application (Jiangsu), which is the first governmental authorized Coordination Innovative Center, IoT in China. He also serves as a referee or expert in multiple national organizations and committees. He has authored and coauthored more than 200 technical papers published in various journals and conferences. Currently, he is leading a big group and multiple funds on IoT and wireless communications with current focus on architecture and enabling technologies for Internet of Things. His research interests include mobile communications, wireless communication theory, and electromagnetic compatibility.